Progress in field-free magnetic imaging on Thermo Scientific transmission electron microscopes

Ricardo Egoavil[1*], András Kovács[2], Pavel Potocek[1,3], Eric Van Cappellen[4], Maria Meledina[1], Dileep Krishnan[1], Zino Leijten[1], Peter Tiemeijer[1], Lynette Keeney[5], Michele Conroy[6], Rafal E Dunin-Borkowski[2], Maarten Wirix[1] and Bert Freitag[1]

[1]Thermo Fisher Scientific, Achtseweg Noord 5, 5651 GG, Eindhoven, The Netherlands
[2]Ernst Ruska-Centre for Microscopy and Spectroscopy with Electrons, Forschungszentrum Jülich, 52425 Jülich, Germany
[3]Saarland University, 66123, Saarbrücken, Germany
[4]Thermo Fisher Scientific, 5350 NE Dawson Creek Drive, Hillsboro, OR 97124, USA
[5]Tyndall National Institute, University College Cork, Cork T12 R5CP, Ireland
[6] Department of Materials, Royal School of Mines, Imperial College London, London, UK

[*] ricardo.egoavil@thermofisher.com

Field-free magnetic imaging using scanning transmission electron microscopy (STEM) enables nanometer- to ångström-scale resolution [1], but routine measurements is often limited by diffraction contrast from bend contours. We report field-free magnetic imaging on Thermo Scientific transmission electron microscopes (TEMs) using a frame-based precession workflow implemented via AutoScript TEM, where programmable control of electron-beam tilt and rotation suppresses diffraction-related effects and enhances magnetic contrast. The approach is demonstrated on representative magnetic materials, including $Nd_2Fe_{14}B$, B20-FeGe, and Fe_3O_4 thin films. Cryogenic measurements and momentum-resolved EELS are also explored under field-free conditions. These results highlight how AutoScript TEM enables automated acquisition strategies, supporting scalable, multimodal characterization workflows for emerging magnetic materials.

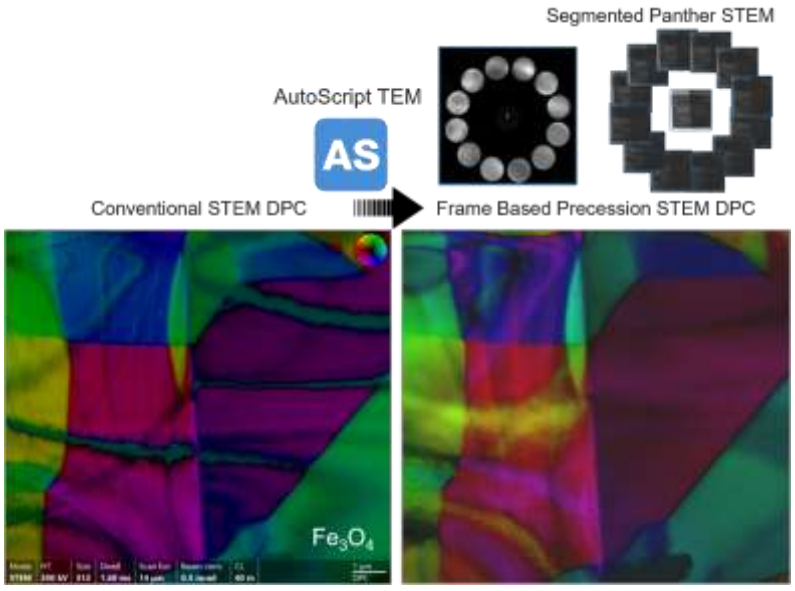

Fig. 1: Field-free imaging of an Fe_3O_4 thin film. (left) Conventional STEM-DPC with diffraction contrast. (right) Frame-based precession STEM-DPC suppressing diffraction contrast.

References:

[1] R. Egoavil et al. Microscopy and Microanalysis, Volume 31, Issue Supplement 1, July 2025, ozaf048.1133. https://doi.org/10.1093/mam/ozaf048.1133.

Development of a C_c/C_s Corrector Based on Hexapole and Quadrupole Fields

Shigeyuki Morishita[1,2,3,4*], Norihiro Okoshi[2], Shunsaku Waki[2], Hironori Tanaka[2], Katsunori Ichikawa[2], Hidetaka Sawada[2], and Angus Kirkland[3,4]

[1] JEOL (U.K.) Limited, 1-2 Silver Court, AL7 1LT, Welwyn Garden City, U.K.
[2] JEOL Ltd., 3-1-2 Musashino, 196-8558, Akishima, Japan
[3] University of Oxford, Department of Materials, Parks Road, OX1 3PH, Oxford, U.K.
[4] Rosalind Franklin Institute, Harwell Science and Innovation Campus, OX11 0QX, Didcot, U.K.

[*]shigeyuki.morishita@jeoluk.com

Spherical and chromatic aberrations are fundamental and inevitable limitations of the lenses used in transmission electron microscopes. Although the spherical aberration correctors have been widely used for high-resolution imaging, chromatic aberration correctors remain limited in number, despite their importance for various applications such as imaging of thick specimens, observation using electron guns with a wide energy spread or a low accelerating voltage, and imaging using objective lenses with large chromatic aberration coefficients. In this study, we have developed a chromatic and spherical aberration corrector based on quadrupole and hexapole fields.

In the developed corrector, thick hexapole fields generate negative spherical aberration as in conventional hexapole-type spherical aberration correctors. To produce negative chromatic aberration, superimposed electric and magnetic quadrupole fields are introduced between the two hexapole fields. The quadrupole quadruplets also function as a transfer doublet for the hexapoles. By using this configuration shown in Figure 1, chromatic and geometric aberrations can be corrected simultaneously. The corrector has been installed in the imaging system of a transmission electron microscope.

Measurements of the residual aberrations indicate that the first-order chromatic aberration was corrected, and the second-order chromatic astigmatism became dominant. The correction of geometric aberrations allows an aberration-free angle of more than 30 mrad. The effect of chromatic aberration correction has been demonstrated by intentionally inducing energy oscillations. Images of gold particles on an amorphous film indicate that clear Thon rings can be obtained under C_c corrected condition even with an energy oscillation of 100 eV as shown in Figure 2. This aberration corrector is expected to significantly improve image quality in cases where chromatic aberration is the dominant limiting factor [1].

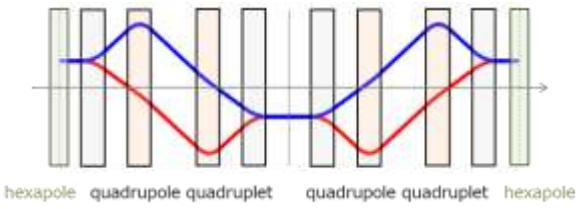

Fig. 1: Optical configuration of the developed C_c/C_s corrector

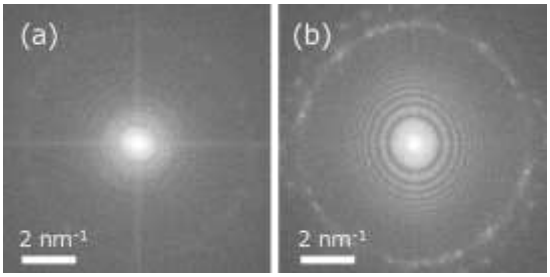

Fig. 2: Fourier transforms of TEM images with an energy oscillation of 100 eV under (a) uncorrected and (b) C_c/C_s corrected conditions.

References:
[1] S. Morishita, *et al*., Ultramicroscopy, accepted (2026).

Exploring electron dose fractionation in TEM for material science applications using the latest generation of fast hybrid pixel detectors

Vavra, Jan[1*], Oveisi, Emad[2], Zambon, Pietro[1], Hemperek, Tomasz[1], Piazza, Luca[1], Meffert, Matthias[1]

[1] DECTRIS AG, Täfernweg 1, 5405, Baden, Switzerland
[2] École polytechnique fédérale de Lausanne (EPFL), Switzerland

[*]jan.vavra@dectris.com

Electron dose fractionation is an established technique in the life-science TEM community, recording individual electron hits at the detector plane is maximizing the amount of useful information that can be extracted with a limited number of electrons. [1] The latest generation of direct electron counting hybrid pixel detectors achieve framerates above 100kHz [2], extend the dose fractionation principle into dose rates closer to the realm of material science TEM. Currents between 1-10 pA can be used for electrons homogenously distributed within a frame as in conventional TEM imaging. Under these conditions, interpretable TEM images can be acquired in less than a second, while retaining information about individual electron hits in individual sub-frames. This acquisition mode allows for sensitive evaluation of sample changes induced by the electron beam or external stimuli. Dose fractionation can further enhance detector DQE [3] and allow for precise drift correction.
In the present work, the detector setup and data processing are guided by a simulated detector response according to Allpix[2] model. [4] Benefits and drawbacks of dose rate fractionation for real-life material science samples are explored; in both imaging and diffraction modes with particular focus on electron damage process for beam sensitive samples and dynamic (in-situ triggered) processes.

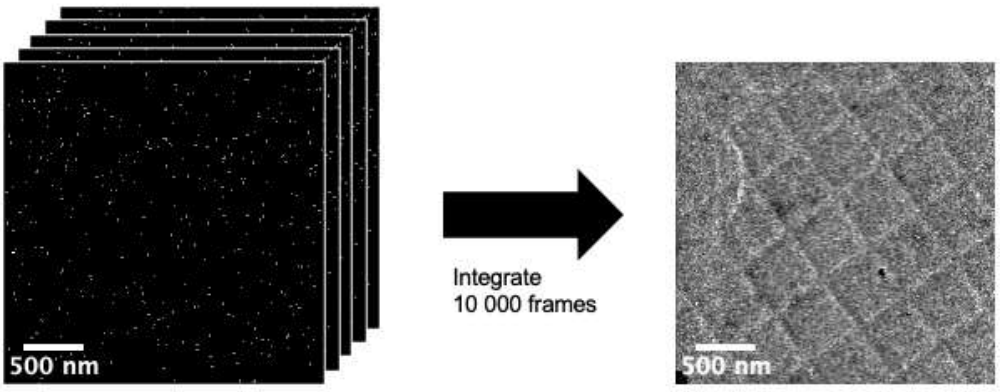

Figure 1. Illustrates the principle of dose fractionation with a fast detector. 10 000 images resolving individual electron events been acquired over the course of 1s with DECTRIS ARINA CZT detector. Dose rate: 130 e/px/s

References:
[1] G. McMullan *et al*, PNAS 120 (2023), 10.1073/pnas.231290512

ATOMIC-RESOLUTION COUNTED EELS ON NON-ABERRATION-CORRECTED MICROSCOPES USING GIF CONTINUUM AND ADVANCED eaSI WORKFLOWS

Saleh Gorji[1*], Liam Spillane[2], Andrew M. Thron[2], Ray Twesten[2], Anahita Pakzad[2]

[1]Ametek GmbH, Gatan+EDAX, Rudolf-Diesel-Str. 16, 64331 Weiterstadt, Germany
[2] Gatan Inc., Pleasanton, 5794 W Las Positas Blvd., USA

[*]saleh.gorji@ametek.com

While aberration correction has greatly improved the spatial resolution of the STEM, the reality of beam-specimen interactions in a typical EELS experiment often means the resolution is limited by the SNR of the data and not by the probe size. Recent advances in direct electron detection and high-speed spectrum imaging workflows maximize the SNR of the collected data enabling atomic-resolution EELS even on non-aberration-corrected TEM/STEM instruments, overcoming traditional limits imposed by drift, sample instability, and detector readout noise. Modern counting cameras such as the K3 and the Stela hybrid pixel detector deliver single-electron sensitivity, negligible read noise, sharp point-spread functions, and extremely high frame rates, allowing dose-efficient spectrum imaging at all accelerating voltages.

Combined with the GIF Continuum platform and eaSI (efficient and synchronized spectrum imaging) technology, these detectors facilitate fully synchronized EELS, EDS, and imaging acquisition while providing automated metadata correlation and live drift correction. Continuous drift correction applied between successive passes removes drift artifacts that would otherwise be present in long, single-scan acquisitions, enabling large-area or atomic-resolution spectrum imaging even during long or dynamic in-situ experiments.

Dose-fractionated EELS acquisition, enabled by high-speed counting detectors, is particularly powerful for both robust and beam-sensitive materials. Due to the low readout noise and high sensitivity of the counting detectors, individual sparsely populated spectra can be sum together to improve the SNR. Instead of long single-pass dwell times, many sparse, low-dose passes are acquired and selectively summed post-collection. This permits removal of compromised passes (beam damage, contamination, drift), and preserves high-fidelity ELNES information by rejecting damaged passes and retaining pristine chemical state information.

These capabilities extend naturally to cryo-EELS. Using Gatan's new liquid-nitrogen cryo holder, atomic resolution can be maintained despite the typically high drift rates at low temperature. Ultra-short pixel times (110–339 µs) minimize beam dose, and increase the frame rate of spectrum image acquisition, helping minimize sample instabilities due to thermal drift. Furthermore, direct detection enables high-quality mapping up to 3000 eV energy range at probe currents as low as 20 pA on an uncorrected 200 kV system.

Together, the combination of counted EELS, dose fractionation, continuous drift correction, and eaSI multimodal acquisition redefines what is achievable on non-aberration-corrected instruments. These workflows enable reliable atomic-resolution EELS on a broad range of materials—including highly beam-sensitive systems—supporting advanced in-situ, cryogenic, and multimodal STEM experiments.

SENSITIVITY AND ROBUSTNESS OF QUANTITATIVE PHASE ANALYSIS AND STRAIN MEASUREMENTS BY PRECESSION-ASSISTED 4D-STEM

Daniel Nemecek[1*], Tomas Moravek[1], Nithin Iyappan[1], Brendan Clarke[1]

[1]Tescan Group, 63700, Brno, Czech Republic

[*]daniel.nemecek@tescan.com

The introduction of fast pixelated detectors with a large dynamic range has revived the advanced methods of electron diffraction for characterization of a broad range of materials and phenomena by analytical scanning transmission electron microscopy [1,2]. Electron diffraction maps (4D-STEM datasets) can now be acquired efficiently from large regions of interest in just several minutes. The quality of acquired diffraction patterns can be substantially improved by beam precession [3], which reduces the deleterious effects of dynamic scattering in the data while increasing the number of detected spots in acquired diffraction patterns. Techniques based on template matching, such as phase-orientation mapping, then become more accurate and robust, especially when several phases are present in the sample. Beam precession also results in more homogeneous intensities of individual diffraction spots which facilitates more accurate determination of their position to the sub-pixel level, making the analytical diffraction methods based on “center-of-mass” measurements, such as strain analysis or differential phase contrast, more accurate and precise.

The power of analytical 4D-STEM measurements enhanced by beam precession with precise microscope alignments and fast data acquisition speeds [4], will be demonstrated on the challenging examples of phase analysis of pleiomorphic materials, such as annealed HZO thin films [5], and strain measurements in advanced Si:SiGe multi-layers and technology nodes.

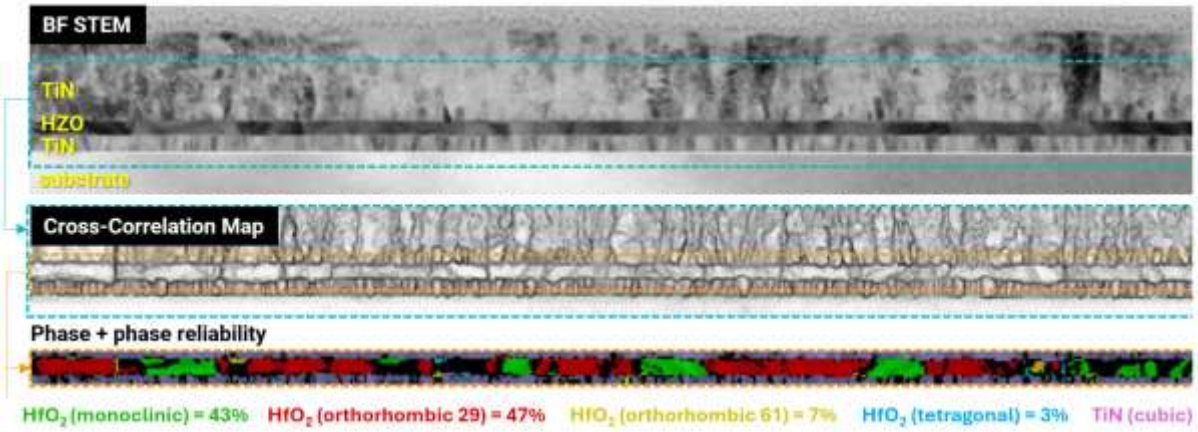

Fig. 1: Example of quantitative phase analysis of grains in an annealed HZO film by 4D-STEM enhanced by precise beam precession [5]. Multiple possible HZO phases were considered and evaluated, including the monoclinic (green) and the orthorhombic (red).

References:

[1] A. Forster, et al., Phil. Trans. R. Soc. A **377**, 20180241 (2019).
[2] C. Ophus, Microsc. Microanal. **25**, 563–582 (2019).
[3] P.A. Midgley, A.S. Eggeman, IUCrJ, **2**, 126 (2015).
[4] D. van der Wal, Microscopy Today, **31**, 15 (2023).
[5] A. Diebold, et al., Microsc. Microanal. **31**, ozaf019 (2025).

STUDYING EXTENDED-RANGE ORDER USING PAIR-ANGLE DISTRIBUTION FUNCTIONS

Rebekka Klemmt[1*], Alan Salek[2], Martin A. Karlsen[3], Dorthe B. Ravnsbæk[1], Andrew V. Martin[2], Espen D. Bøjesen[1,4]

[1]Center for Sustainable Energy Materials, Department of Chemistry, Aarhus University, Langelandsgade 140, 8000 Aarhus, Denmark
[2]School of Science, RMIT University,124 La Trobe Street, Melbourne, VIC 3000, Australia
[3]Beamline P02.1, PETRA III, Deutsches Elektronen-Synchrotron DESY, Notkestraße 85, Hamburg 22607, Germany
[4]Interdisciplinary Nanoscience Centre, Aarhus University, Gustav Wieds Vej 14, 8000 Aarhus, Denmark

[*]rekl@chem.au.dk

The lack of long-range order challenges the important characterization of the extended-range order of disordered materials with conventional crystallographic methods based on diffraction. Alternative methods have to be used for investigating disordered materials. A well-established example is the use of pair distribution function (PDF) analysis which provides crucial information on average interatomic distances. Although PDF is a valuable tool to study the structure of disordered materials, it has the limitation that meaningfully different structural models might result in identical PDFs, as angular arrangements between atom pairs are only described indirectly [1]. Hence, advanced methods are needed which are able to describe the angular arrangements in the extended-range order of disordered materials.
A method which has this ability is the pair-angle distribution function (PADF) analysis [2]. It characterizes the atomic structure in terms of two atomic pair distances (r, r') and the angle (θ) of three-atom and four-atom pairs. PADF is a method still in its infancy and has mainly been used to characterize the short-range order of materials. With our work, we explore the possibilities of using PADF for elucidating the extended-range order of disordered materials at the example of highly sp^2-hybridized disordered carbons. In the case of disordered carbon, the information-rich PADF can be used to separately study the disorder within and in between graphite-like stacked layers, which is not possible in comparable ways using PDF analysis. The PADF analysis approach will contribute to an enhanced understanding of the structure of disordered carbons and other layered disordered materials.

References:
[1] P. M. Maffettone, W. J. K. Fletcher, T. C. Nicholas, V. L. Deringer, J. R. Allison, L. J. Smith, A. L. Goodwin, *Faraday Discuss.* **255**, 311-324 (2025).
[2] A. V. Martin, *IUCrJ* **4**, 24-36 (2017).

Microwave-cavity-based Ultrafast Electron Microscopy and Spectroscopy

Jom Luiten[1,2*], Yuri Janson[1]

[1]Eindhoven University of Technology, Department of Applied Physics, Groene Loper 3, 5612 AE, Eindhoven, NL
[2]Doctor X Works B.V., De Zaale 11, 5612 AJ, Eindhoven, NL

[*]o.j.luiten@tue.nl

At Eindhoven University of Technology (TU/e) we have developed a method for doing *Ultrafast Transmission Electron Microscopy (UTEM)* at 75 MHz repetition rate with ~100 fs temporal resolution [1]. The method is based on the use of a dual-mode 3.000/3.075 GHz resonant microwave *deflection* cavity, operating in TM_{110}-mode (Fig. 1), which sweeps the beam across a Lissajous pattern (Fig. 2) with a 75 MHz repetition frequency. Combined with a Timepix-3 direct electron camera this technique allows the measurement of the arrival time statistics of the 200 keV electrons with sub-ps temporal resolution, revealing sub-Poissonian behavior at the shortest time scales [2]. Employing a small aperture at the center of the Lissajous pattern to chop the electron beam in combination with a synchronized Toptica femtosecond fiber laser, we recently performed pump-probe experiments of the PINEM effect at 75 MHz with 300 fs resolution (to be published). Pump-probe experiments on 2D quantum materials are presently being done. We are preparing the installation of a 6 GHz microwave cavity, operating in TM_{010}-mode, which, combined with a BOM-PD synchronization scheme, will enable $\leq$10 fs temporal resolution by pulse compression. In addition, we are investigating the possibility of using the 6 GHz TM_{010}-cavity to *stretch* the pulses, resulting in reduction of the uncorrelated energy spread. A second 3 GHz TM_{010}-cavity, positioned downstream, will subsequently serve to *de-chirp* the stretched pulse, realizing pulsed lossless monochromation. In this way *Ultrafast EELS* can be realized at 60 keV at 75 MHz repetition rate, with $\leq$100 meV energy resolution and ~1 ps temporal resolution, at an average current of ~1 pA. These numbers may be further improved by longitudinal aberration correction [3].

Fig. 1: TM_{110} dual mode deflection cavity.

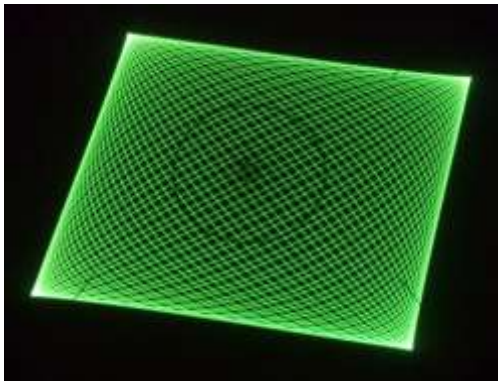

Fig. 2: Lissajous pattern on the detector.

References:
[1] W. Verhoeven et al., Ultramicroscopy **188**, 85 (2018).
[2] S. Borrelli et al., Phys. Rev. Lett. **132**, 115001 (2024).
[3] Y. Janson, MSc thesis, Eindhoven University of Technology (2025), to be published.

The UltraCold Electron Source: Principle, Recent Developments and Potential Applications

Julius Huijts[1*], Ameya Patwardhan[1], Jom Luiten[1]

[1]Eindhoven University of Technology, Applied Physics, De Groene Loper 19, 5612AP, Eindhoven, The Netherlands

[*]j.v.huijts@tue.nl

Ultrashort electron pulses enable the study of ultrafast processes in nature. Such pulses can be generated in an electron microscope by gating the electron emission with an ultrashort laser pulse [1], or by chopping a continuous electron beam with an RF cavity [2], but the resulting pulses typically contain less than one electron on average. Alternatively, it is possible to generate pulses with sufficient charge for single-shot imaging [3], but with a significant loss of coherence causing substantial image degradation.

An interesting alternative is offered by the UltraCold Electron Source, which has been under development in the past two decades at the Eindhoven University of Technology. [4, 5, 6]. Here, electron pulses are created through photoionization of laser-cooled atoms. Careful tuning of the photoionization laser wavelength allows minimizing the transverse temperature of the electron bunch to 10 K, maximizing transverse coherence. The generated electron pulses are of ultrashort duration [7] and can have charges up to a femtoCoulomb, placing this technology between the two extremes introduced above.

On this poster I will explain the basic principle of the technique and present recent developments, including a novel design implementation combining DC and RF acceleration to achieve a 100 keV electron energy that is currently being manufactured. I will also discuss potential applications and limitations of this unique technology.

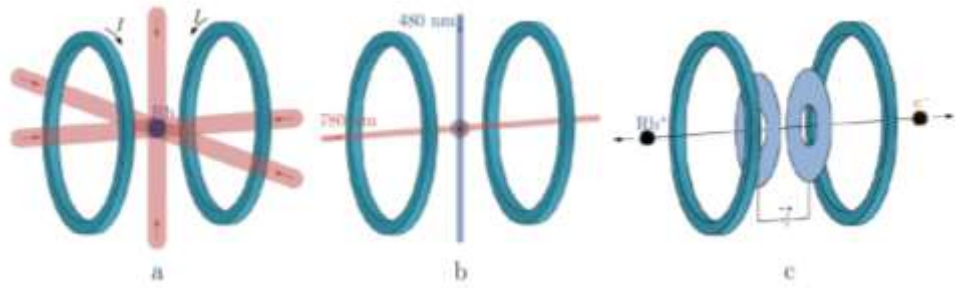

Fig. 1: Schematic illustration of the principle of the ultracold electron source. (a) Laser-cooling and trapping of atoms. (b) Photo-ionization of the laser-cooled atoms. (c) Acceleration of the electron bunch by a DC electric field. Image from: [8]

References:
[1] A. Gahlmann *et al.*, Phys. Chem. Chem. Phys. **10**, 2894-2909 (2008)
[2] W. Verhoeven *et al.,* Ultramicroscopy **188**, 85-89 (2018)
[3] T. LaGrange *et al.*, Micron **43**, 1108-1120 (2012)
[4] B.J. Claessens *et al.,* Phys. Rev. Lett. **95**, 164801 (2005)
[5] J.G.H. Franssen *et al.* Phys. Rev. Acc. Beams **22**, 023401 (2019)
[6] J.V. Huijts, O.J. Luiten, http://arxiv.org/abs/2510.09889 (2025)
[7] T.C.H. de Raadt *et al.*, Phys. Rev. Lett. **130**, 205001 (2023)
[8] J.G.H. Franssen *et al.*, Struct. Dyn. **4**, 044010 (2017)

Python-Based Data Processing for Quantitative Analysis of Focused Ion Beam (FIB) Tomography

Junbeom Park[1*], Tobias Mehlkoph[1], Adolé Imelda Akue-Goeh[1], Pritam Chakraborty[1,2], Jean-Pierre Poc[1,2], André Karl[1], Eva Jodat[1], Shibabrata Basak[1], Rüdigar-A. Eichel[1,2]

[1]Forschungszentrum Jülich, Institute of Energy Technologies – Fundamental Electrochemistry (IET-1), Wilhelm-Johnen-Straße, 52425, Jülich, Germany
[2]Institute of Physical Chemistry, RWTH Aachen University, Landoltweg 2, 52074, Aachen, Germany

[*]j.park@fz-juelich.de

Understanding the structure and properties of materials is crucial in various fields such as batteries, fuel cells and water electrolysis [1]. Three-dimensional (3D) tomography is a powerful imaging technique that allows for the visualization of internal structures and their relationships to neighboring structures. Focused ion beam (FIB) tomography is a type of 3D tomography that is particularly suitable for analyzing cutting-edge materials with nm to µm sized features, like microporous structures in catalyst layer for energy applications.

However, handling FIB tomography datasets can be challenging due to their large size, typically consisting of hundreds of images. Additionally, FIB tomography datasets often contain artifacts such as image drifting caused by long acquisition times and curtaining effects resulting from ion beam damage. Furthermore, extracting quantitative information such as material composition and porosity requires advanced data processing techniques like segmentation.

To address these challenges, we have developed a Python-based data processing procedure for quantitative analysis of FIB tomography [2]. Our procedure is designed to be versatile and applicable to most FIB tomography datasets with minimal modification. The procedure consists of three main steps: 1) pre-processing to organize and reshape the dataset, 2) segmentation to distinguish and label featured areas, and 3) data reconstruction to calculate and visualize quantitative information. We will present our Python-based data processing procedure using two energy-related applications: proton exchange membrane water electrolyzer and solid oxide fuel cell.

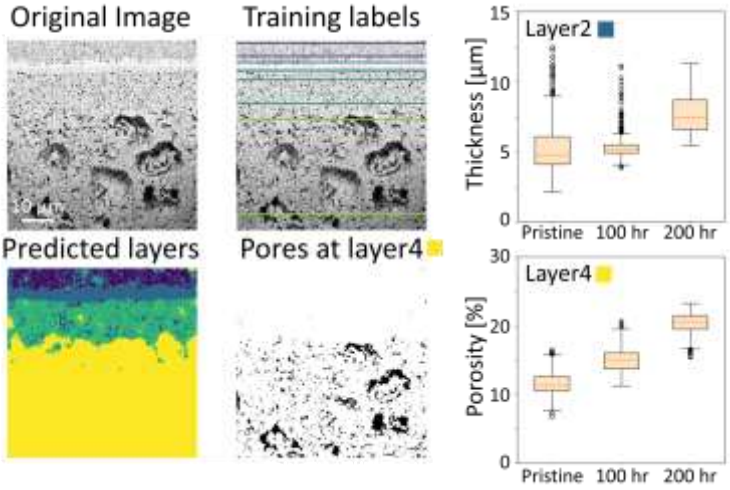

Fig. 1: FIB tomography data processing result

References:
[1] V. Wilke et al. Electrochemical Science Adv. 5 (2025) e202400036
[1] P. Chakraborty et al. Nano Today 61 (2025) 102649

Electron microscopy and trams: Towards a friendly coexistence

Thomas Schachinger[1*], Ulrich Bette[2], Thomas Brückl[3], Stephanie Manz[4], Andreas Randacher[3], Wolfang Emmer[5], Thomas Mallits[6]

[1]TU Wien, USTEM, Wiedner Haupstraße 8-10, 1040, Vienna, Austria
[2]IfB Institut für Beeinflussungsfragen, Konrad-Adenauer-Str. 57, 42111, Wuppertal, Germany
[3]WIENER LINIEN GmbH & Co KG, I64 Anlagenmanagement, Erdbergstraße 202, 1030, Vienna, Austria
[4]TU Wien, Atominstitut Quantummetrology, Stadionallee 2,1020, Wien, Austria
[5]ESC Engineering & Services GmbH, Nikolaiplatz 4, 8020, Graz, Austria
[6]IES Institut f. Elektrotechnik u. Sicherheitswesen Ziviltechniker GmbH, Gastgebgasse 27, 1230, Vienna, Austria

[*]thomas.schachinger@tuwien.ac.at

State-of-the art transmission electron microscopes' (TEM) performance is suffering from a multitude of environmental disturbances like mechanical vibrations and slowly varying magnetic fields, putting stringent threshold limits on these environmental factors, e.g., ≤ 25 nT for magnetic fields [1]. At the same time choosing remote and thus "quiet" areas is typically no option, as TEM labs are traditionally placed in- or close by city centers, demanding reasonable access to public transport. Tram lines represent an efficient solution but they are DC powered, drawing 500-1000 A of current, causing large scale low-frequency, magnetic field disturbances, potentially reducing imaging- and analytical performance of TEMs, see Fig. 1a. Even though there are active and passive compensation systems at the instrument side available, they are limited in performance when it comes to strong field gradients, costly and difficult to retrofit. Similar on the tram side, battery- and ground-level power supply based systems can reduce the field emissions but they are also costly and demand specialized tramcars.
An effective and economic solution is a passive system that strongly reduces the area of the current loop produced by the catenary and the rails using a clever arrangement of a bypass cable and additional supply points on the catenary [2], see Fig. 1b. By adopting this Ansatz to the dense urban setting of Vienna with the additional implementation of a rail track mass-spring vibration isolation a maximum field of 20 nT per tram at a distance of 100 m can be achieved, see Fig. 2b. This 10–20-fold reduction compared to no compensation has been verified by extensive finite element simulations and calibration tests, see Fig. 2a.
By implementing this "Viennese" variant of a passive field reduction system for tram lines urban public transport demands no longer interfere with researchers' desire for electromagnetic quietness.

a)

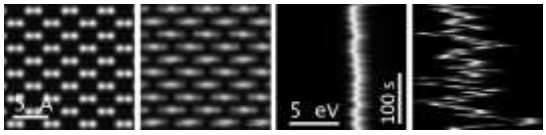

b)

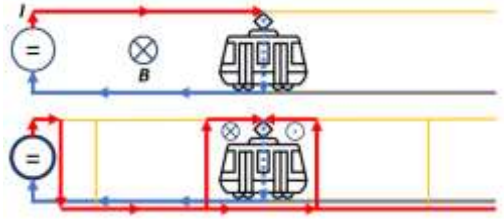

Fig. 1: a) TEM image distortions and energy shifts caused by near-DC magnetic fields and b) tram field reduction system principle.

a)

b)

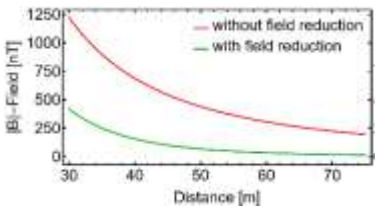

Fig. 2: a) 3D-FEM simulation result for the new "Linie 18" extension (blue: <20 nT), b) field distribution as a function of distance to rails.

References:
[1] Muller et al., Ultramicroscopy **106,** 1033–1040 (2006).
[2] Pieter Kruit et al., eb Elektrische Bahnen **118,** 100- 118 (2020) Heft 6.

LOW-DOSE IMAGING AND ELECTRON DIFFRACTION

Haipei Shao[1,2*]

[1] Institute of Materials Research and Engineering, Agency for Science, Technology and Research, 2 Fusionopolis Way, 138634, Singapore
[2] Department of Chemistry, Faculty of Science, National University of Singapore, 3 Science Drive 3, 117543, Singapore

[*]haipei.shao@gmail.com

Electron microscopy of beam-sensitive and structurally complex materials requires tailored experimental strategies that balance spatial resolution, chemical sensitivity, and electron dose. In this contribution, I present four independent microscopy studies, each addressing a distinct methodological challenge across imaging, diffraction, spectroscopy, and data-driven reconstruction.

Low-dose imaging. I conduct low-dose imaging of covalent organic frameworks (COFs), a class of highly beam-sensitive crystalline polymers. By optimizing S/TEM acquisition and dose management, polycrystalline domains and topologies are directly visualized while preserving structural integrity, enabling real-space insight into mesoscale ordering.

Three-dimensional electron diffraction (3D ED). I present the structure solution of a newly discovered one-dimensional material. The novel crystal structure is solved ab initio from nanoscale crystals, highlighting the power of 3D ED as a low-dose reciprocal-space technique for materials that are unsuitable for conventional single-crystal X-ray diffraction.

Electron energy-loss spectroscopy (EELS). I report on atomic-resolution EELS of Geminal-atom catalysis. By combining aberration-corrected STEM with optimized spectroscopic acquisition, individual atomic species are directly identified, providing unambiguous chemical verification of isolated active sites at the single-atom level.

AI for Microscopy. I introduce a data-driven approach to electrostatic potential reconstruction using segmented annular dark-field images. This method employs physically constrained simulations to train a neural network that bypasses analytical inversion, offering improved robustness against specimen mis-tilt, thickness variations, and breakdown of weak-phase assumptions.

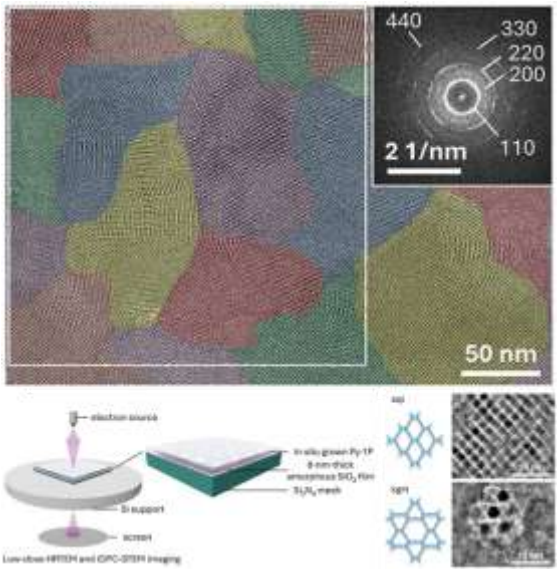

Fig. 1: Low-dose imaging of COF polycrystal.

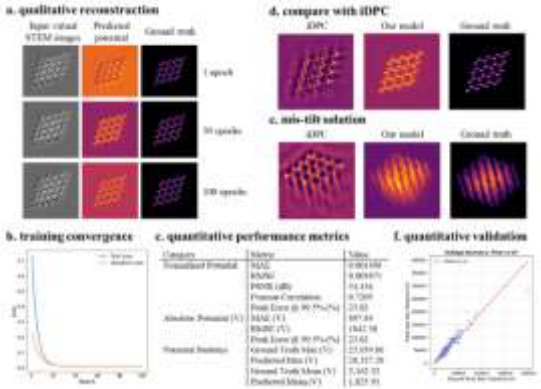

Fig. 2: Data-driven method for potential reconstruction.

RESISTIVE SWITCHING OF INDIVIDUAL TiO_2 NANOPARTICLES STUDIED BY OFF-AXIS ELECTRON HOLOGRAPHY

Janghyun Jo[1*], Vadim Migunov[1,2], Dirk Oliver Schmidt[3], Helmut Soltner[4], Ulrich Simon[3], Miyoung Kim[5], and Rafal E. Dunin-Borkowski[1]

[1]Ernst Ruska-Centre for Microscopy and Spectroscopy with Electrons, Forschungszentrum Jülich, 52425 Jülich, Germany
[2]Central Facility for Electron Microscopy, RWTH Aachen University, 52074 Aachen, Germany
[3] Institute for Inorganic Chemistry, RWTH Aachen University and JARA – Fundamentals of Future Information Technologies, 52074 Aachen, Germany
[4]Central Institute of Engineering, Electronics and Analytics (ZEA-1), Forschungszentrum Jülich, 52425 Jülich, Germany
[5] Department of Materials Science and Engineering and Research Institute of Advanced Materials, Seoul National University, Seoul 08826, Korea

[*] j.jo@fz-juelich.de

Resistive switching phenomena in complex oxides have attracted significant interest for next-generation non-volatile memory applications owing to their high speed, low power consumption and cost effectiveness. Memristive or resistive random access memory devices are leading candidates to replace flash memory across a diverse range of fields [1, 2]. Recently, nanoparticles have been adopted as switching materials, serving both as functional components for device scaling and as model systems for elucidating resistive switching mechanisms at the nanoscale [3, 4]. Here, we investigate the origin of resistive switching in individual TiO_2 nanoparticles, which are examined under an applied electrical bias using *in situ* transmission electron microscopy (TEM) and off-axis electron holography.

In order to study resistive switching mechanisms in real time, current-voltage (*I*-*V*) measurements were performed *in situ* in the TEM using a Nanofactory specimen holder. Off-axis electron holography was applied simultaneously. The technique can be used to record maps of projected electrostatic potential with nm spatial resolution [5], providing insight into the presence of local changes in potential and charge density and the formation of conducting nanofilaments during switching. We observed reproducible bipolar switching of individual nanoparticles that were electrically addressed in the TEM using a moveable electrical probe. *I*-*V* curves measured from individual nanoparticles were correlated with projected electrostatic potential and charge density measurements. Abrupt changes in potential and charge density were observed when the current increased significantly during a voltage sweep. Comparisons between experimental projected potential maps and simulations suggest that a localized conducting path is created and annihilated within the nanoparticle during switching. Charge accumulation was detected along this local path, suggesting that its presence is associated with SET and RESET processes.

In summary, non-volatile bipolar resistive switching was observed in individual TiO_2 nanoparticles. Correlation between phase images measured using off-axis electron holography, electrostatic potential simulations and charge density maps confirmed that resistance changes are localized within the nanoparticles, which are attributed primarily to the drift of oxygen vacancies and their subsequent accumulation and depletion near interfaces.

References:

[1] M. Lanza et al., Science, **376**, 1066 (2022).
[2] D. V Christensen et al., Neuromorphic Comput. Eng. **2**, 022501 (2022).
[3] E. Goren et al., Appl. Phys. Lett., **105**, 143506 (2014).
[4] D. O. Schmidt et al., Small, **11**, 6444 (2015).
[5] M. R. McCartney et al., Annu. Rev. Mater. Res., **37**, 729 (2007).

Determination of the bowing of spontaneous polarization in $In_xGa_{1-x}N$ using off-axis electron holography and electrostatic modeling

Qiangjan Lan[1]*, Keyan Ji[1], Michael Schnedler[1], Rafal E. Dunin-Borkowski[1], Philipp Ebert[1]

[1]Ernst Ruska Centrum (ER-C-1), Forschungszentrum Jülich GmbH, 52425 Jülich, Germany

*q.lan@fz-juelich.de

Polarization engineering has played an important role in advancing III-nitride semiconductor devices over recent decades. However, the exact magnitude and orientation of polarization remain highly debated, as significant discrepancies persist among different theoretical approaches and experiments. A major source of this inconsistency lies in the difficulty of directly measuring internal polarization fields at the nanoscale, especially across heterointerfaces like $In_xGa_{1-x}N$/GaN.

In this work, we resolve this problem by combining off-axis electron holography with surface potential calibration [1] and self-consistent electrostatic modeling [2] to directly measure quantitative polarization changes at $In_xGa_{1-x}N$/GaN interfaces. By integrating these methods with strain measurements from STEM imaging, we separated the total polarization change into its piezoelectric and spontaneous components. The experimental results reveal a strongly nonlinear dependence of spontaneous polarization on indium composition: at low indium concentrations it can be described by a parabolic form, while over the full composition range a cubic dependence is required. This nonlinear bowing accounts for the systematic overestimation of polarization in theoretical models assuming linear or quadratic trends. Crucially, we demonstrate that only a layered hexagonal reference phase—not the commonly used zincblende phase—accurately captures the observed spontaneous polarization behavior. These results establish a consistent theoretical framework for group-III nitrides and clarify the composition dependence of polarization in the technologically important $In_xGa_{1-x}N$ alloy.

References:

[1] K. Ji, M. Schnedler, Q. Lan, J.-F. Carlin, R. Butté, N. Grandjean, R. Dunin-Borkowski, and P. Ebert, Ultramicroscopy 264, 114006 (2024).
[2] M. Schnedler, R. E. Dunin-Borkowski, and Ph. Ebert, Phys. Rev. B 93, 195444 (2016).

Ag/Au contact electrification measured using off-axis electron holography

Yan Lu[1*], Yufan Zhang[2,3], Benjamin Klingebiel[4], Tobias Binninger[2], Rafal E. Dunin-Borkowski[1]

[1]Ernst Ruska-Centre for Microscopy and Spectroscopy with Electrons (ER-C-1), Forschungszentrum Jülich GmbH, 52428 Jülich, Germany
[2]Theory and Computation of Energy Materials (IET-3), Institute of Energy Technologies, Forschungszentrum Jülich GmbH, 52425 Jülich, Germany
[3]Chair of Theory and Computation of Energy Materials, Faculty of Georesources and Materials Engineering, RWTH Aachen University, 52062 Aachen, Germany
[4]Photovoltaik (IMD-3), Institute of Energy Materials and Devices, Forschungszentrum Jülich GmbH, 52425 Jülich, Germany

[*]y.lu@fz-juelich.de

Contact electrification occurs as a result of charge exchange when two surfaces come into contact, due to a difference in their work functions. Off-axis electron holography is a powerful transmission electron microscopy technique that can be used to map local variations in electron optical phase shift, which are sensitive to electrostatic potentials and magnetic fields. In the absence of magnetic fields, a recorded phase image is proportional to the electrostatic potential projected in the electron beam direction. Here, we study contact electrification between a Ag nanocube (NC) and a Au substrate. The phase shift and charge distribution are also simulated using orbital-free density functional theory (OF-DFT).

Figures 1a-c show an electron hologram of a 70 nm Ag NC on a Au substrate, the reconstructed phase shift after subtracting a vacuum reference wave, and corresponding equiphase contours with a spacing of 2π/8 radians, respectively. Figure 1d shows the phase shift of a different 70 nm Ag NC, from which the phase decays into vacuum from the Ag NC. Figure 1e shows an OF-DFT calculation of the simulated phase shift , which is in close agreement with the experimental results. The simulation reveals the charge distribution in the system, as shown in Fig. 1f. Positive charge is located on the Ag NC and at the interface, while negative charge is located on the Au surface. This approach offers a platform for studying how contact electrification depends on material composition and structure.

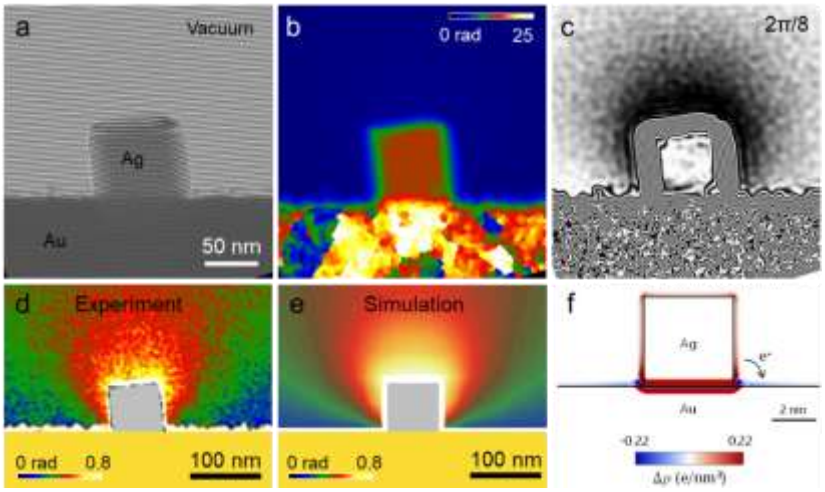

Figure 1 (a) Off-axis electron hologram of a 70 nm Ag nanocube. (b) Corresponding phase shift. (c) Corresponding equiphase contours of spacing 2π/8 radians. (d) Phase shift of a different 70 nm Ag nanocube. (e) OF-DFT simulated phase shift. (f) Charge distribution.

Electron beam charging at *p-n* junctions: Interplay of electron dose and charge carrier dynamics

Dorothee S. Rosenzweig[1*], Michael Schnedler[1], Rafal E. Dunin-Borkowski[1], and Philipp Ebert[1]

[1]Forschungszentrum Jülich, Ernst-Ruska Centre for Electron Microscopy, Wilhelm-Johnen-Straße 1, 52428, Jülich, Germany

[*]d.rosenzweig@fz-juelich.de

Electron beam charging is a well-known limitation in quantitative off-axis electron holography of semiconductor *p-n* junctions, but its influence on measured phase shifts is typically not addressed in quantitative analyses. [1]
In order to quantify electron-dose dependent charging, temperature-resolved measurements at a *p-n* junction were performed as a function of electron dose (2 - 7 C m^{-2} s^{-1}) and sample temperatures (23 - 490°C). The phase contrast at *p-n* junctions decreases monotonically with increasing electron dose, and show a systematic temperature-dependent offset, with higher temperatures yielding consistently larger phase contrast values over the entire electron dose range. The largest holographic phase contrast is obtained at the smallest electron dose and the highest temperature. In contrast, electron holographic phase measurements on an *n/n*$^+$ δ-doped layer within the same sample show no dose-dependent behavior.
The temperature dependence of the dose response of the phase contrast of *p-n* junctions in conjunction with the dose independence of *n/n*$^+$ δ-doped layer indicates that beam charging is governed by the balance between beam-induced charge generation and temperature-dependent charge carrier transport and recombination, such that identical electron doses can produce different phase shifts depending on thermal conditions. These results demonstrate that beam charging systematically reduces the measured potential difference at *p-n* junctions relative to the nominal built-in potential and that charge carrier dynamics play a crucial role in screening beam-induced charge. Explicit consideration of all experimental parameters influencing electron beam charging is therefore essential for quantitative electron holography.

References:
[1] Niermann, Ultramicroscopy **276,** 114191 (2025)

ATOMIC-SCALE INTERFACE ANALYSIS OF NbTiN TRILAYER SUPERCONDUCTING JUNCTIONS

Hayden C. Barry[1*], Nicholas Dugan[2], Jordan A. Hachtel[3], Michael Cyberey[2], Kory Burns[1]

[1]Department of Materials Science and Engineering, University of Virginia, Charlottesville, VA, 22904, United States
[2]Department of Electrical Engineering, University of Virginia, Charlottesville, VA, 22904, United States
[3]Center for Nanophase Materials Sciences, Oak Ridge National Laboratory, Oak Ridge, TN 37831, United States

[*]haydencbarry@virginia.edu

Superconducting digital-logic circuits require precise control of multilayer materials at the atomic scale to optimize efficiency in processing data. Unfortunately, conventional characterization utilizing optical probes fail to resolve individual interfaces within vertically stacked heterostructures without spatial averaging. The application of aberration-corrected scanning transmission electron microscopy (STEM) coupled with energy-filtered scanning nano diffraction 4D-STEM can achieve atomic-resolution analysis of NbTiN/barrier/NbTiN trilayer systems, while also spatially resolving impurities embedded in the barrier layer, which are an increasingly important metric for assessing device performance in novel superconducting junctions. In this presentation, we first correlate local electron energy loss spectroscopy (EELS) measurements and STEM images to map impurities driving interface instability with bulk-scale device measurements. Next, we introduce the concept of energy-filtered scanning nanodiffraction 4D-STEM, which greatly reduces the background noise and isolates our incoherent elastically scattered electrons for enhanced structural and chemical profiling. Here, spectrum images are generated and structurally deconvolved based on their diffraction signals to discriminate atomically sharp NbTiN/Si and NbTiN/GaN interfaces from any intermixed regions. The combined acquisition with core-loss EELS allows for the detection of subtle variations in nitrogen coordination number and oxidation state across the barrier layers, where distortion is the highest. Importantly, by combining atomic-scale structural information with chemical sensitivity, this approach establishes a strong basis for understanding how interface quality influences the device performance critical to superconducting junction efficiency, and opens the pathways for the rational design of superconducting tunnel junctions with minimal dissipation and enhanced detector sensitivity.

Leveraging Machine Learning for Advanced Nanoscale X-ray Analysis: Unmixing Multicomponent Signals and Enhancing Chemical Quantification

Hui Chen[1*], Duncan T.L. Alexander[2], Cécile Hébert[2]

[1]Catalan Institute of Nanoscience and Nanotechnology (ICN2), CSIC and BIST, Campus UAB, Bellaterra, 08193 Barcelona, Catalonia, Spain
[2]Electron Spectrometry and Microscopy Laboratory (LSME), IPHYS, EPFL, Lausanne, Switzerland

[*]hui.chen@icn2.cat

Energy dispersive X-ray (EDX) spectroscopy in the transmission electron microscope is a key tool for nanomaterials analysis, providing a direct link between spatial and chemical information. However, using it for precisely determining chemical compositions presents challenges of noisy data from low X-ray yields and mixed signals from phases that overlap along the electron beam trajectory. To address these limitations, we develop PSNMF (non-negative matrix factorization based pan-sharpening) [1], an innovative machine learning approach that enhances STEM-EDX analysis by simultaneously separating overlapping phases and reconstructing a high-quality dataset. By leveraging the Poisson nature of EDX spectral noise and binning operations, PSNMF retrieves high-quality phase spectral and spatial signatures via consecutive non-negative matrix factorizations (NMF), enabling precise and robust dataset reconstruction.

We validate PSNMF using synthetic datasets with varying noise levels, as well as experimental STEM-EDX data from nano-mineralogical samples and Au-Cu2O catalytic nanoparticles. These datasets represent two major categories of samples commonly analyzed in STEM-EDX: 1) lamellae of uniform thickness that are prepared from bulk materials using ion beam milling and/or mechanical thinning; 2) nanostructures of irregular thickness that are supported on amorphous carbon films. Our results demonstrate that PSNMF not only obtains accurate phase signatures, outperforming the benchmark method, NMF, in identifying minor phases within complex materials, but also reconstructs datasets with significantly lower noise and higher fidelity than the benchmark denoising method, principal component analysis (PCA), particularly for trace element quantification. The superior phase decomposition accuracy and enhanced clarity of the denoised elemental maps highlight PSNMF's strong potential for improving STEM-EDX analytics across a variety of nanoscience domains.

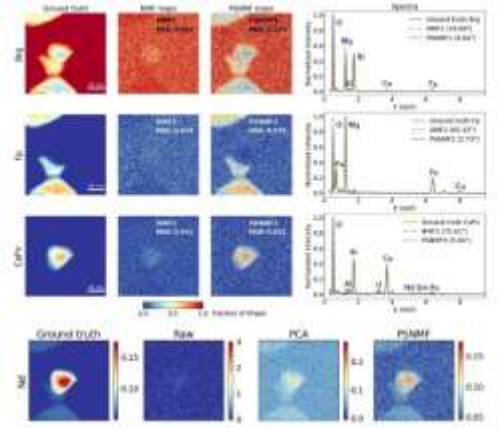

Fig. 1: PSNMF applied to a simulated data set having a very low SNR (average of 18 X-ray counts per pixel), compared to standard NMF for phase identification and to PCA for data set denoising.

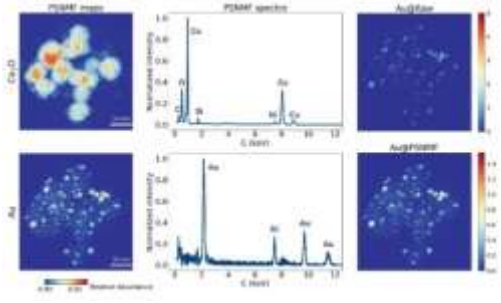

Fig. 2: PSNMF applied to an experimental 512 × 512 pixel data set that was acquired from Au−Cu2O nanoparticles supported on a carbon film.

References:

[1] H. Chen, D. T. L. Alexander, C. Hébert, Nano Lett. **24**, 10177–10185 (2024).

GENERALIZED ELECTRON-DRIVEN NON-EQUILIBRIUM SYSTEMS for IN-SITU MICROSCOPY

Vinayak P. Dravid[1*]

Department of Materials Science and Engineering, Northwestern University, Evanston, IL, USA

[*]v-dravid@northwestern.edu

Transformative advances in electron sources, aberration corection, and detectors have elevated electron microscopy to unprecedented spatial, temporal, and spectral resolution. Yet the full potential of these developments remains unrealized for *in-situ* experiments. Conventional windowed chips impose dominant limitations through multiple scattering, dielectric losses, and poorly controlled coupling between electrons, matter, and energy—fundamentally constraining quantitative interpretation.

GENESIS is an experimental framework enabled by the ultrathin (UT) membrane platform, which removes these bottlenecks. The UT architecture employs ultrathin, mechanically robust, and electrical/thermal-transparent membranes that dramatically reduce scattering while preserving environmental realism. Beyond fluidic operations, a single-membrane implementation functions as a combined electron microscopy/scanning probe microscopy (EM/SPM) substrate, enabling high-throughput nanoparticle discovery via Megalibrary methodologies. The fluidic UT platform supports high pressures and enables quantitatively interpretable imaging, diffraction, and spectroscopy.

Representative GENESIS demonstrations include real-time imaging and EELS of radical-driven polymerization, where bond formation and chain growth are tracked concurrently. Complementary time-resolved diffraction+spectroscopy resolve subtle phase transitions, transient distortions and non-equilibrium ordering inaccessible in conventional geometries.

At a unifying level, GENESIS transforms *in-situ* microscopy as a driven, open system operating far from equilibrium, where measured electron–matter interaction trajectories encode work, dissipation, hidden and excess entropy and fluctuations rather than static free energies. This perspective provides experimental access to non-equilibrium statistical relations that link microscopic dynamics to macroscopic response, for example,

$$\langle e^{-\beta W} \rangle = e^{-\beta \Delta F}.$$

Figure: Schematic illustration of UT chip as a miniature "*playground'* for quantum and fluctuation phenomena.

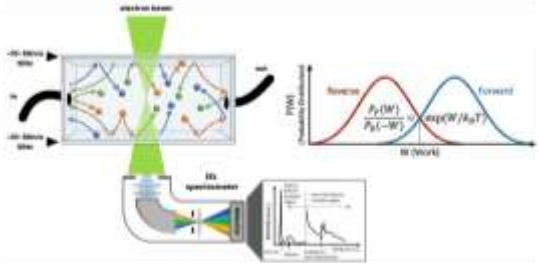

By integrating ultrathin interfaces with controlled electrical, thermal, and optical driving, GENESIS provides a general platform for interrogating low-energy excitations governing chemical selectivity and phase stability. Rather than marginally extending existing methods, GENESIS enables modern electron optics to be fully realized for quantitatively interpretable, driven non-equilibrium systems.

References:

[1] F. M. Ross, Nature Nanotechnology 10, 343–346 (2015)

[2] O. L. Krivanek et al., Nature 514, 209–212 (2014).

[3] Dravid, V. P. et al., Science Advances (2024), doi:10.1126/sciadv.adj6417.

[4] Dravid, V. P. et al., Proceedings of the National Academy of Sciences (2024), doi:10.1073/pnas.2408277121.

MAGNETIC DOMAIN STRUCTURES IN LAMELLAE OF THE VAN DER WAALS MAGNETS Fe_3GeTe_2 and Fe_3GaTe_2

Eva Duft[1*], Lidia Kibkalo[1], Nikolai S. Kiselev[2], Rafal E. Dunin-Borkowski[1], Joachim Dahl Thomsen[1]

[1] Ernst Ruska-Centre for Microscopy and Spectroscopy with Electrons, Forschungszentrum Jülich, Wilhelm-Johnen-Straße, 52428 Jülich, Germany
[2] Peter Grünberg Institute, Forschungszentrum Jülich, Wilhelm-Johnen-Straße, 52428 Jülich, Germany

[*]e.duft@fz-juelich.de

Van der Waals (vdW) magnets such as Fe_3GeTe_2 (FGT) and the room temperature ferromagnet Fe_3GaTe_2 (FGaT) are promising candidates for applications in next-generation spintronic devices. Here, we use Lorentz transmission electron microscopy (LTEM) and off-axis electron holography to measure the magnetic domain width W in cross-sectional lamellae of FGT and FGaT of height h and thickness $t \approx 200$ nm viewed perpendicular to the crystallographic c-direction. Figure 1 shows a representative LTEM image, on which the sample dimensions, magnetic domain width, and magnetization directions of the domains are marked. Our measurements reveal that FGaT has larger values of W at large values of h compared to FGT (Fig. 2), qualitatively in agreement with the Kittel model [1]. Mumax[3] [2] micromagnetic simulations performed on the JUWELS Booster [3] using the saturation magnetization M_s, perpendicular anisotropy K_u and exchange stiffness A_{ex} as adjustable parameters support these results. We also investigated the effect of lamella thickness t by comparing the height-dependent domain width in cross-sectional lamellae with results obtained from exfoliated plan-view flakes with lateral sizes of several µm. Our results highlight the limitations of the Kittel model and provide an improved understanding of thickness-dependent domain formation in laterally-confined vdW magnets.

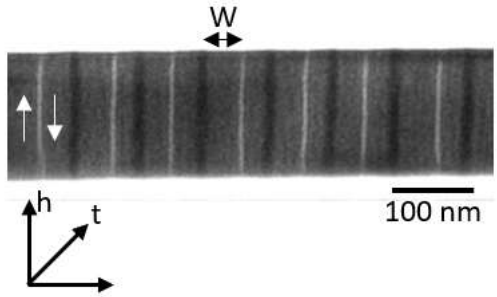

Fig. 1: Representative LTEM image of a cross-sectional lamella of FGaT. The lamella dimensions h and t and the domain width W is indicated. The white arrows indicate the magnetization direction.

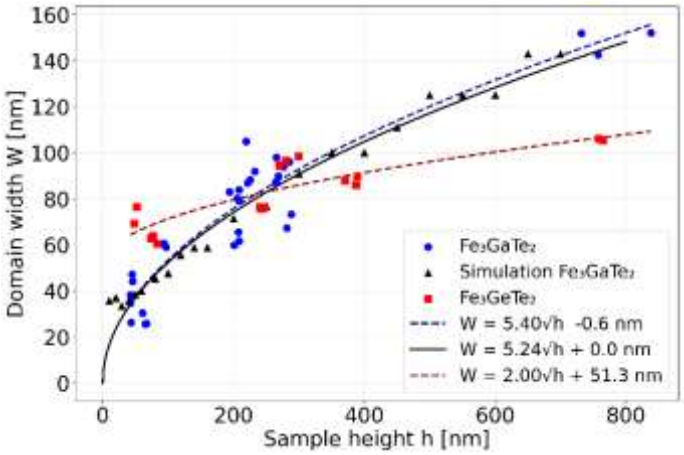

Fig. 2: W plotted against h for FGT and FGaT. Experimental data (circles and squares) and micromagnetic simulation results for FGaT (triangles) using M_s = 475 kA/m, K_u = 180 kJ/m^3 and A_{ex} = 2.8 pJ/m are shown alongside fits to the Kittel model (dashed lines: experiment; solid line: simulation).

References:
[1] C. Kittel, Phys. Rev. **70**, 965-971 (1946)
[2] A. Vansteenkiste et al., AIP Advances **4**, 107133 (2014)
[3] Jülich Supercomputing Centre, Journal of Large-Scale Research Facilities, A183 (2021)

Direct observation of the Verwey transition in magnetite

András Kovács[1*] and Rafal E. Dunin-Borkowski[1]

[1]Ernst Ruska-Centre for Microscopy and Spectroscopy with Electrons, Forschungszentrum Jülich, Jülich, Germany

[*]a.kovacs@fz-juelich.de

Magnetite (Fe_3O_4, cubic spinel, space group 227) undergoes two magnetic transitions. One is a ferrimagnetic-to-paramagnetic transition, which takes place at the Curie temperature (865 K). The other is the so-called Verwey transition, a metal-to-insulator transition that takes place at 125 K. This first order transition is associated with a spontaneous intercorrelated change in lattice symmetry, electronic and magnetic properties. Despite extensive research over almost a century, several fundamental questions about its mechanism remain unresolved. Here, we use *in situ* (scanning) transmission electron microscopy ((S)TEM) techniques to study the Verwey transition in thin films of single crystalline magnetite prepared using focused ion beam thinning. The sample temperature was controlled using liquid-nitrogen-cooled TEM holders (Gatan and DENS Lighting Arctic). (S)TEM imaging and electron diffraction (Fig. 1(a)) were used to monitor structural transformations of the films from the cubic to monoclinic crystal structure, which were typically accompanied by the formation of stacking faults. Both conventional (S)TEM and Lorentz mode were used to assess the influence of an external magnetic field on the Verwey transition. Magnetic domain walls were studied using Fresnel defocus imaging (Fig. 1(b,c)) and off-axis electron holography (EH). An experiment was also performed to study the impact of the Verwey transition on the saturation magnetisation of Fe_3O_4 nanocubes, based on magnetic phase shift images reconstructed from EH experiments and on their analysis using a model-based inversion algorithm. The experimental findings were compared with micromagnetic simulations.

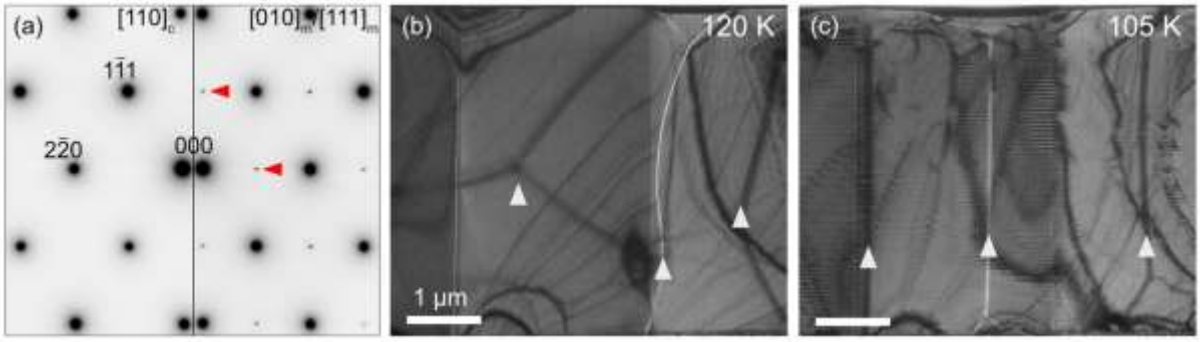

Figure 1. (a) Electron diffraction patterns recorded from cubic (left) and monoclinic (right) Fe_3O_4 at room temperature and 95 K, respectively. Superlattice reflections are marked by red arrowheads. (b, c) Fresnel defocus images recorded at 120 and 105 K, respectively, with magnetic domain walls marked by white arrowheads. The fine horizontal bands of contrast in (c) are stacking faults.

References:
[1] The authors are grateful to R. Egoavil and M. Meledina (ThermoFisher Scientific) and to G. Pivak and M. Andersen (DENSsolutions) for support and contributions to the experiments.

MICROSTRUCTURAL DYNAMICS REVEALED BY ELECTRON BEAM TECHNIQUES

Yoshie Murooka[1*]

[1]University of Liverpool, School of Engineering, Brownlow Hill, L69 3GH, Liverpool, UK

[*]y.murooka@liverpool.ac.uk

Fast dynamics occurring at the microscopic scale have been advanced over decades using electron beam and high-frequency techniques alongside laser technology. This advancement involves not only fundamental physical processes within samples, but also external stimuli to the sample, the sample environment, and electron optics.

In electron microscopy, for example, major scientific themes are to elucidate microscopic dynamics and structures. The techniques such as a fast chopper, a photoelectron source using short-pulse lasers and two-dimensional digital detectors [1] enabled the combination of high spatial-, momentum-, and energy-resolutions with time resolution [2].

Over the past 20 years, ultrafast laser technology has dramatically increased the temporal resolution of electron diffraction and microscopy [3,4,5]. Using femtosecond pulsed electron beams, for example, light-induced structural dynamics of nanoparticles [6] and surface structures [7], charge transfer at substrate surfaces [8], light control of magnetic structures [9], visualisation of surface plasmon polaritons [10], and light-matter interactions based on quantum processes [11] have been clarified in both reciprocal space and real space.

At the University of Liverpool, STEM imaging utilising compressed sensing has been developed [12]. This enables observation of beam-sensitive samples, can reduce acquisition time, and allows low dose observations. In addition, RUEDI (Relativistic Ultrafast Electron Diffraction and Imaging) was proposed, utilising MeV beams from accelerator technology [13,14]. This aims to observe ultrafast phenomena in thick samples within both real space and reciprocal lattice space, which has previously been challenging.

At the poster, I would like to discuss new opportunities in micro-dynamics alongside advances in external stimulation techniques, environmental techniques, and electron optics.

References:

[1] D. McMullan, et al. Inst. Phys. Conf. Ser. No.98: EMAG-MICRO 89, (1989), p.55-58.
[2] Y. Murooka and J. Yuan, Proc. ICEM 13-PARIS (1994) p.751-752.
[3] B.J. Siwick, et al., Science 302 (2003) 1382.
[4] H. Ihee, et al., Science 291 (2001) 458-462.
[5] T. LaGrange, et al., Ultramicroscopy 108 (2008) 1441–1449.
[6] C.-Y. Ruan, et al., Nano Letters 7, 1290-1296 (2007).
[7] R.K. Raman, et al., PRL 101, 077401 (2008).
[8] R. A. Murdick, R. K. Raman, Y. Murooka, and C.-Y. Ruan, Phys. Rev. B 77, 245329 (2008).
[9] G. Berruto, et al., Phys. Rev. Lett. 120, 117201 (2018).
[10] L. Piazza, et al., Nature Comm. | 6:6407 | DOI: 10.1038/(2015).
[11] A. Feist, et al., Nature 521 (2015), 200-203.; V. Grillo, et al., Nature Comm. 8 (2017)15536.
[12] D. Nicholls, et al., Ultramicroscopy 233 (2022) 113451.
[13] N. D. Browning, et al., Microsc. Microanal. 28 (Suppl 1), (2022), p.2764
[14] Y. Murooka, et al. Micro. & Micro., 29 (2023) pp. 1487-1488. ISSN 1431-9276.
[15] The author would like to thank the entire RUEDI team including science teams and EPSRC/UKRI

EXPLORING THE INFLUENCE OF Cr ON BOND CHARACTERISTICS IN $(Fe,Cr)_2B$

Akhil G. Nair[1*], Chanchal Ghosh[2], Arup Dasgupta[2]

[1]Ernst Ruska-Centre for Microscopy and Spectroscopy with Electrons, Forschungszentrum Jülich, 52425 Jülich, Germany
[2]Indira Gandhi Centre for Atomic Research, A CI of Homi Bhabha National Institute, Kalpakkam 603102, Tamil Nadu, India

[*]a.nair@fz-juelich.de

Boron-added steels are valued for their hardness, corrosion and wear resistance, and high neutron-absorption capacity, making them ideal for applications such as spent fuel storage. In modified 9Cr1Mo steel, boride forms as $(Fe,Cr)_2B$. While Fe_2B-based composite steels are well-studied, the specific role of Cr in $(Fe,Cr)_2B$ remains less understood. This study examines atomic-level changes in $(Fe,Cr)_2B$ and their effect on bonding characteristics using density functional theory (DFT), supported by aberration-corrected microscopy and spectroscopy. For DFT modeling, the $(Fe,Cr)_2B$ supercell was structurally relaxed using spin-polarized plane augmented wave (PAW) calculations. Norm-conserving calculations with Optimized Norm-Conserving Vanderbilt (ONCV) pseudopotentials were then performed, and the results were analyzed using the Critic2 software to compute Bader's delocalization indices (DI). The results revealed longer Cr-B bond lengths than Fe-B bond lengths, indicating a change in bonding characteristics. The increased ionicity in $(Fe,Cr)_2B$ relative to Fe_2B correlates with reduced stiffness in the elastic regime, confirmed via nanoindentation testing. Experimental validation involved Extended Electron Energy Loss Fine Structure (EXELFS) spectroscopy to measure bond lengths. Energy loss spectra for Fe and Cr were processed to derive radial distribution functions (RDFs), which matched DFT-predicted bond lengths. High-angle annular dark-field (HAADF) and integrated Differential Phase Contrast (iDPC) imaging were also used to cross-validate projection lengths against DFT-relaxed structures. The study concludes that Cr incorporation alters bonding in $(Fe,Cr)_2B$, influencing mechanical properties by increasing ionicity and reducing stiffness [1]. These findings enhance the understanding of chromium's role in boride steels, with implications for their performance in advanced applications.

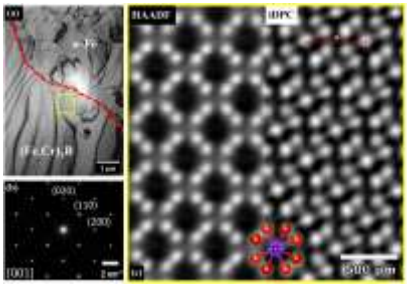

Fig. 1: (a) BF image of boride and ferrite. (b) SADP along [001] of boride. (c) HAADF and iDPC showing Fe dumbbells around B, overlaid with a $(Fe,Cr)_2B$ model (Fe: red, Cr: green, B: purple).

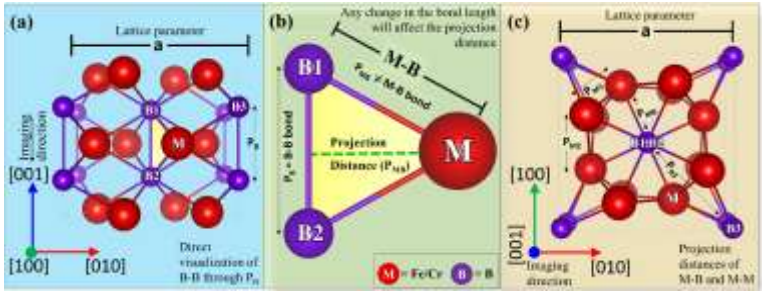

Fig. 2: (a) M_2B structure along [100] showing the atoms considered for the projection distance calculation. (b) Relation between projection distance and bond length. (c) M_2B structure along [001] ZA (also the imaging zone for the present work) shows the projection distances considered in the present work.

References:
[1] AG. Nair et al., Physica B: Condensed Matter **715**, 417596 (2025).

SHEARING OF CHEMICALLY COMPLEX VANADIUM CARBIDE NANOPRECIPITATES IN MICROALLOYED STEELS

Amir Sabet Ghorabaei[1*], Bart J. Kooi[1]

[1]Zernike Institute for Advanced Materials, University of Groningen, Nijenborgh 3, 9747 AG Groningen, The Netherlands

[*]amir.sabet.ghorabaei@rug.nl

Vanadium carbide (VC) nanoprecipitates are generally regarded as non-shearable obstacles in the context of precipitation strengthening mechanisms in microalloyed steels [1]. However, recent electron microscopy studies have revealed evidence of sheared interphase-precipitated VC within the ferritic matrix of such steels [2]. Since embedded nanoprecipitates are difficult to probe at atomic resolution due to matrix interference, this study employs an optimized carbon extraction replica method [3] to isolate VC nanoprecipitates, both before and after tensile testing, for atomic-resolution structural and chemical analysis using scanning transmission electron microscopy (STEM) techniques. The VC nanoprecipitates are found to be chemically complex and non-stoichiometric, showing co-incorporation of iron and manganese (Fig. 1). Sheared fibrous and elliptical VC precipitates are identified in the sample subjected to the highest logarithmic strain (Fig. 2). It is proposed that the presence of carbon vacancies combined with the co-segregation of iron and manganese into the multi-component VC lattice lowers the critical stress required for precipitate shearing. These findings contribute to a deeper understanding of nanoscale precipitation strengthening mechanisms in microalloyed steels.

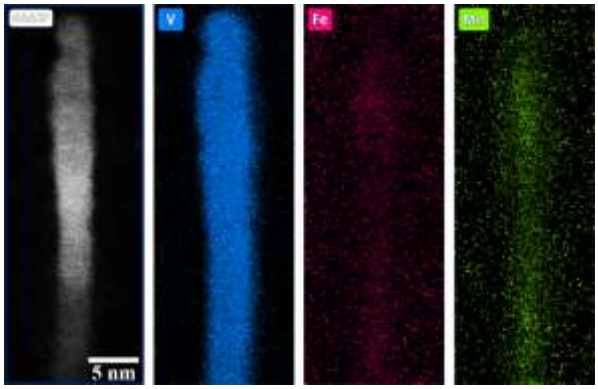

Fig. 1: Chemical complexity of fibrous interphase VC nanoprecipitates.

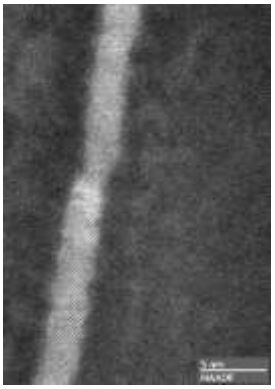

Fig. 2: Multiple shearing of fibrous VC nanoprecipitates.

References:
[1] N. Kamikawa et al., Acta Mater. 83 (2015) 383–396.
[2] E. Pereloma et al., Mater. Res. Lett. 8 (2020) 341–347.
[3] A.S. Ghorabaei, B.J. Kooi, J. Mater. Res. Technol. 30 (2024) 6418–6429.

Spin reorientation effect in a thin film of the kagome magnet Fe_3Sn_2

L. Sagenschneider[1*], A. Kovács and R.E. Dunin-Borkowski[1]

[1]Ernst Ruska-Centre for Microscopy and Spectroscopy with Electrons, Forschungszentrum Jülich, 52425 Jülich, Germany

[*]l.sagenschneider@fz-juelich.de

Fe_3Sn_2 is a kagome-type magnet, which has attracted significant attention due to its unique properties, including an anomalous Hall effect, flat electron bands near the Fermi energy and massive Dirac fermions [1]. Fe_3Sn_2 has a centrosymmetric rhombohedral structure, in which Fe-Sn bilayers alternate with Sn layers along the crystallographic c-axis, resulting in uniaxial magnetic anisotropy. In bulk Fe_3Sn_2, a spin reorientation effect, involving a change from easy-axis to easy-cone and to easy-plane anisotropy, has been reported [1]. Here, we use transmission electron microscopy (TEM) to study the spin reorientation effect in a thin film of Fe_3Sn_2 that hosts dipolar skyrmions. Electron-transparent specimens were fabricated following a standard lift-out method using focused ion beam sputtering in a dual beam system. Specimens were prepared with thicknesses of between ~100 and ~250 nm. Magnetic imaging was carried out using the Fresnel mode of Lorentz TEM down to liquid He temperature (<10 K) in magnetic-field-free conditions. A lattice of dipolar skyrmions with type I and type II structures was observed after applying a magnetic field of ~600 mT perpendicular to the specimen using the objective lens of the microscope at room temperature. After cooling to 95 K using a liquid-nitrogen-cooled holder (Gatan 636), we observed the elimination and transformation of the dipolar skyrmions (Fig. 1), which merged and formed elongated structures. The sample was then examined at 5 K using a liquid-helium-cooled holder (condenZero). At this temperature, stable dipolar skyrmions were observed together with in-plane magnetic domains. After magnetic saturation, the magnetic configuration was found to be predominantly in-plane, in accordance with the presence of dominant easy-plane anisotropy in Fe_3Sn_2 at 5 K.

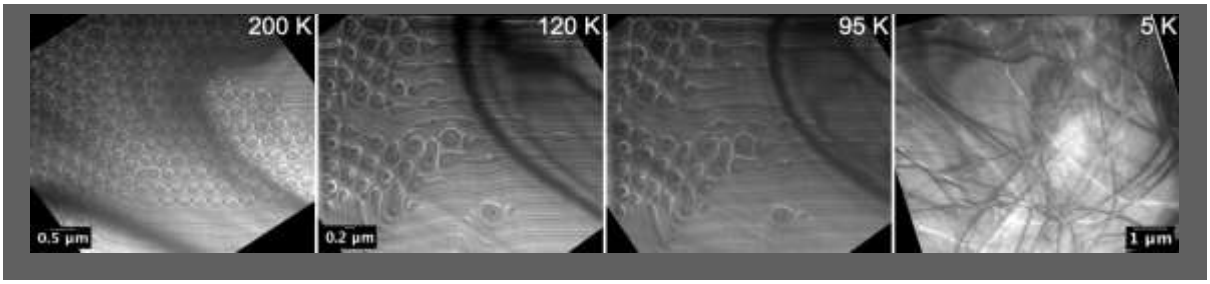

Fig. 1: Lorentz TEM images showing the evolution of dipolar skyrmions at specimen temperatures of 200, 120 and 95 K. The image recorded at 5 K shows an in-plane magnetic domain state formed after magnetic saturation.

References:
[1] L. Prodan et al., Easy-cone state mediating the spin reorientation in the topological kagome magnet Fe_3Sn_2, Phys. Rev. B 111, 184442 (2025).
[2] The authors are grateful to L. Prodan and I. Kezsmarki for providing Fe_3Sn_2 single crystals and to L. Kibkalo and D. Kong for support in specimen preparation.

Dominant role of defect-induced strain in the first-order transition of $Fe_{50}Rh_{50}$

Nan Wang[1*], Qianqian Lan[1], Alex Aubert[2], Nicolas J. Peter[3], Rafal E Dunin-Borkorwski[1]

[1]Ernst Ruska-Centre for Microscopy and Spectroscopy with Electrons, Forschungszentrum Jülich GmbH, 52425 Jülich, Germany
[2]Functional Materials, Institute of Material Science, Technical University of Darmstadt, 64287 Darmstadt, Germany
[3]Institute of Energy Materials and Devices, Forschungszentrum Jülich GmbH, 52425 Jülich, Germany

[*]na.wang@fz-juelich.de

First-order magnetostructural transitions enable external control over material properties through coupled changes in spin, lattice, and electronic degrees of freedom [1]. In these systems, lattice strain crucially influences phase behavior by modifying the free-energy landscape and selectively stabilizing competing phases across wide temperature range and stress regimes. Understanding how strain dictates phase stability and transition pathways is thus essential for both fundamental materials physics and the design of magneto-functional devices. $Fe_{50}Rh_{50}$, a model system, exhibits a sharp antiferromagnetic (AFM) to ferromagnetic (FM) transition near room temperature, accompanied by an abrupt lattice expansion of approximately 1% [2]. This strong magnetoelastic coupling has motivated extensive efforts to tune the transition in FeRh through external pressure, chemical modification, and epitaxial strain engineering.

Previous studies have shown that substrate, interface, and surface-induced strain and film thickness can significantly modulate the AFM-FM transition temperature in FeRh[3]. However, a key limitation in current research is the absence of direct spatial correlation between localized strain fields and magnetic nucleation events at the nanoscale. Here, we investigate the coupling between local strain and the AFM-FM phase transition by combining *in situ* off-axis electron holography over a wide temperature range with 4D-STEM strain mapping in focused-ion-beam-prepared $Fe_{50}Rh_{50}$ lamellae. By directly correlating local strain distributions with magnetic domain nucleation and evolution, we demonstrate that tensile strain accumulation associated with defect-mediated strain fields governs the onset and spatial progression of the FM phase. Furthermore, we show that fabrication-induced damage plays a critical role in modulating transition temperatures and efficiency of nano-sized FeRh. These findings deepen our understanding of mechanisms underlying first-order phase transitions and offer a valuable basis for designing functional magnetic materials for future nano-sized spintronic applications.

References:
[1] S. B. Roy, Journal of Physics: Condensed Matter **25**, 183201 (2013).
[2] M. R. Ibarra, P. A. Algarabel, Physical Review B **50**, 4196-4199 (1994).
[3] C. Gatel et al, Nature Communications **8**, 15703 (2017).

ON COOLING-RATE DEPENDENT EUTECTOID INTERFACE DEVELOPMENT IN TI-7.5CU

J.T. Pürstl[1,2*], Z.H. Fisher[3], A. Genc[2], A.J. Clarke[3,4] and D.S. Gianola[2]

[1]Forschungszentrum Jülich, ER-C-1, Wilhelm Johnen Str., 52428 Jülich
[2]University of California, Santa Barbara, Santa Barbara, CA 93116, USA
[3]Colorado School of Mines, Golden, CO 80401, USA
[4]Los Alamos National Laboratory, Los Alamos, NM 87545, USA

j.puerstl@fz-juelich.de

Understanding interface structure in eutectoid transformations is critical for designing high-strength Ti-Cu alloys, particularly those produced by additive manufacturing. However, the hcp-Ti/tetragonal-Ti_2Cu eutectoid interface characteristics under different cooling conditions have remained incompletely resolved [1,2]. Of interest are cooling-rate dependent morphological changes at fast cooling rates, which lead to ultrahigh strength [3]. This study employs a multi-modal TEM approach combining HR-STEM, 4D-STEM, and EDS mapping (Fig. 1) to investigate interface development in Ti-7.5Cu samples processed at 2 K/s and 150 K/s.

EDS and 4DSTEM mapping reveal a fully partitioned stoichiometric eutectoid regardless of cooling rate. HR-STEM further reveals a fully coherent interface, however with a distinct faceted morphology with alternating terraces parallel to the 0001_{hcp} and 001_{tet} planes. This morphology arises from the crystallographically constrained cooperative growth of hcp-Ti via the quasi-displacive Pitsch-Schrader transformation of 0001_{hcp} and Ti_2Cu through layer-wise ordering of 001_{tet} planes from the parent bcc crystal.

The interface structure differs markedly between cooling rates: fast cooling produces frequent (001)Ti_2Cu terrace steps (~45° overall habit plane), while slow cooling exhibits predominantly $(0001)_{hcp}$ segments with reduced step density. This cooling-rate dependence reflects the competition between transformation kinetics (favoring Ti_2Cu-controlled growth) and interfacial energy minimization (favoring lower-energy hcp-Ti-controlled interfaces).

Both growth processes maintain fully coherent interfaces, allowing interfacial growth to proceed regardless of cooling rate. This is distinct from pearlite growth in steels, where the growth of incoherent austenite/ferrite and austenite/cementite eutectoid interfaces is eventually bypassed by martensite. The pronounced nanoscale interface serration observed under fast cooling conditions may further explain significant strengthening in additively manufactured Ti-Cu alloys.

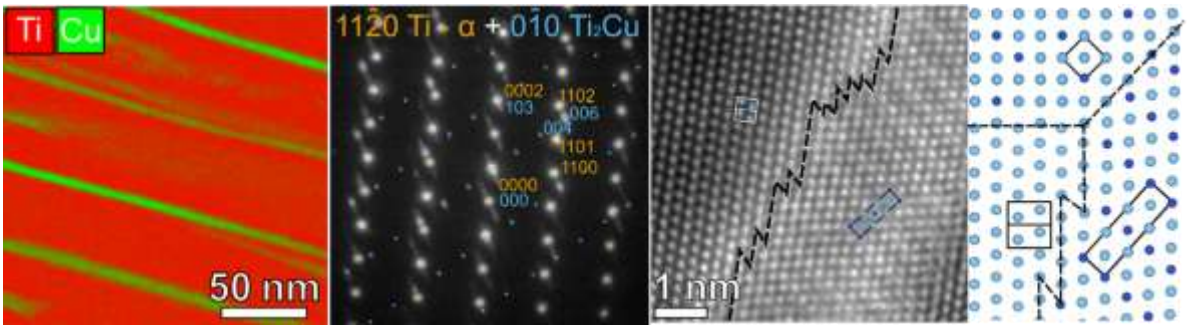

Fig. 1: Combined EDS, 4DSTEM and HR-STEM analysis of fast cooled sample, signifying full eutectoid decomposition with a distinct terrace morphology along interfaces.

References:
[1] P. Mukhopadhyay et al., Metall. Trans. A 10 (1979) 1071-1084.
[2] H. Donthula et al., Acta Mater. 168 (2019) 63-75.
[3] D. Zhang et al., Nature 576 (2019) 91-95.

HYBRID TUNABLE PLASMONIC DEVICES USING GOLD AND VANADIUM DIOXIDE

Rostislav Řepa[1*], Vlastimil Křápek[1], Michal Horák[1], Jiří Liška[1], Jiří Kabát[1], Peter Kepič[1], Tomáš Šikola[1]

[1] Brno University of Technology, Technická 2896, 616 69, Brno, Czech Republic

[*]Rostislav.Repa@vutbr.cz

The lateral arrangement of self-assembled VO_2 nanoparticles and lithographically defined gold nanostructures is presented as a suitable platform for hybrid tunable plasmonic devices. Vanadium dioxide (VO_2) exhibits a metal–insulator transition near room temperature (68 °C), enabling tunable plasmonic functionalities. However, devices based solely on VO_2 suffer from high optical absorption and limited chemical stability [1].

Here, we combine high-quality nanocrystalline self-assembled VO_2 particles [2] with gold nanostructures patterned by electron beam lithography in a lateral arrangement [Fig. 1(a)]. This approach exploits the tunability of VO_2 and the high conductivity of gold, while lithography is applied only to gold to avoid damage to VO_2 and maintain design flexibility. The lateral configuration further reduces the VO_2 volume, contributing to improved device quality.

We demonstrate two tunable devices based on this platform: (1) Electric–magnetic switches, where either an electric or magnetic hot spot is generated following Ref. [3]. Such switches are promising for THz spectroscopy of magnetic transitions [4], to which they can introduce a temporal resolution or facilitate non-linear spectroscopy by promoting either electric or magnetic transitions. (2) Resonance-energy switches, where the energy of the plasmon resonance is controlled, with potential application in fine tuning thermochromic smart windows. Both devices are characterized by analytical electron microscopy, particularly electron energy loss spectroscopy [Fig. 1(b)], and by electrodynamic simulations.

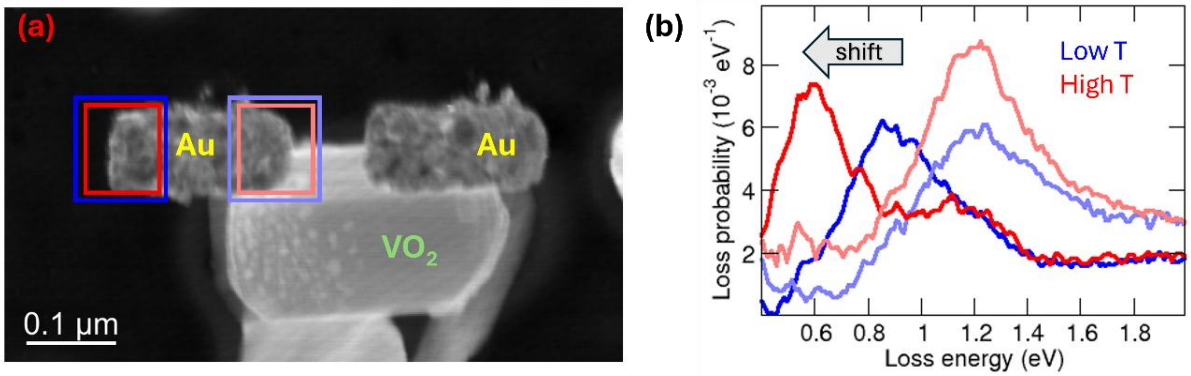

Fig. 1: (a) Annular dark-field image of the resonance-energy switch. A VO_2 nanoparticle and gold nanorods are indicated. (b) Electron energy loss spectra of the same switch taken at the low temperature where VO_2 is insulating (blue) and at the high temperature where VO_2 is metallic (red). The energy shift observed for one of the plasmon resonances is indicated with a gray arrow. The color of the spectra corresponds to the color of the squares in panel (a) indicating the regions where the spectra were retrieved.

References:
[1] J. Krpenský et al., Nanoscale Adv., **6**, 3338-3346 (2024).
[2] M. Horák et al., arXiv:2408.11972 (2024).
[3] V. Křápek et al., Nanophotonics **9**, 623 (2020).
[4] L. Tesi et al., Small Methods **5**, 2100376 (2021).

Crane and Pike: Together they guide

Jakob Ruickoldt[1*], Petra Wendler[1]

[1]Institute for Biochemistry and Biology, University of Potsdam, Am Neuen Palais 10, Potsdam, Germany

[*]jakob.ruickoldt@uni-potsdam.de

The quality of the ice layer embedding the sample is the crucial factor for the success of a cryo-EM data collection. While the quality is largely influenced by global factors like protein concentration, humidity or blotting time, it is also influenced by the local microscopic environment on the grid depending on e.g. the roughness of the blotting paper, the bending angle of the grid or its orientation while plunging. Thus, sometimes extensive screening of the grid is necessary to optimize the data collection.
To streamline the screening procedure, we have developed a GUI called CryoCrane (correlate atlas 'n' exposures) that allows the visualization of the exposure coordinates on the atlas of the grid. Within this GUI we have implemented CryoPike (pick intelligently from kryo-em exposures) – a collection of neural networks trained for cryo-EM micrograph rating. The neural networks were trained on micrographs rated by human experts based on their appearance and power spectrums labelled with the CTF-fit extent calculation in downstream image processing. All neural-networks are small ensuring that the predictions can keep Furthermore, the user can train a neural network – AtlasPike - within CryoCrane based on the atlas images and the scores predicted by CryoPike. AtlasPike predicts the expected score on the atlas with up to 1 µm-resolution enabling a data-based recommendation for the data collection.

CryoCrane is available free of charge on github (https://github.com/jruickoldt/CryoCrane) and runs on Windows, Linux and MacOS.

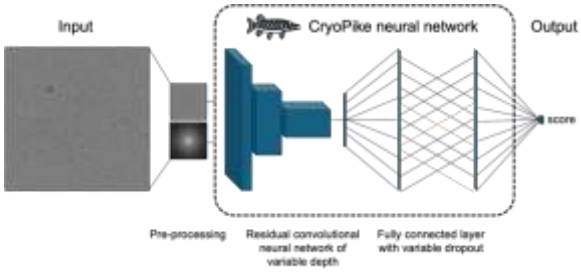

Fig. 1: Workflow of the CryoPike neural network.

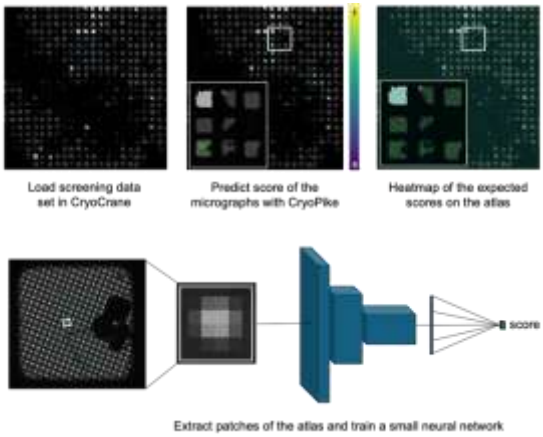

Fig. 2: Workflow for the AtlasPike neural network

The structure-based assembly mechanism of the mitochondrial respiratory chain

Ahad Ali Kazmi[1,2], Irene Vercellino[1,2*]

[1]Ernst Ruska-Centre for Microscopy and Spectroscopy with Electrons (ER-C), Structural Biology (ER-C-3), Forschungszentrum Jülich GmbH, 52428 Jülich, Germany
[2]Heinrich Heine University Düsseldorf, Department of Chemistry, 40225 Düsseldorf, Germany

i.vercellino@fz-juelich.de

The mitochondrial respiratory chain is a set of enzymes involved in the conversion of energy from food to ATP, a molecule that can be used to fuel cellular processes. Since the respiratory chain enzymes are large protein complexes, formed by over 100 proteins overall, an important open question in Bioenergetics is how these respiratory chain complexes are assembled[1]. The importance of this process is highlighted by the myriad of neurodegenerative and cardiological diseases that occur when proper assembly is perturbed[2].

The baker's yeast, *Saccharomyces cerevisiae*, is an established model organism for mitochondrial research due its ability to utilize respiration or fermentation for growth. This enables the genetic manipulation of the respiratory chain complexes for structural purposes, which results in the disruption of mitochondrial respiration, without causing cell death. By using single particle cryo-electron microscopy (cryo-EM), we were able to visualize different assembly intermediates of the yeast respiratory chain complexes. We were also able to visualize how these intermediates assemble into higher-order structures called supercomplexes, known to be the physiological state in which the respiratory chain enzymes exist in the mitochondrial membrane[3]. These assembly mechanisms revealed in *S.cerevisiae* are a promising starting point for understanding general strategies of respiratory chain assembly in other respiring eukaryotes.

References:
[1] I. Vercellino and L. A. Sazanov, "The assembly, regulation and function of the mitochondrial respiratory chain," *Nature Reviews Molecular Cell Biology*, vol. 23, no. 2, pp. 141–161, Feb. 2022, doi: 10.1038/s41580-021-00415-0.
[2] E. Fernandez-Vizarra and M. Zeviani, "Mitochondrial disorders of the OXPHOS system," *FEBS Letters*, vol. 595, no. 8, pp. 1062–1106, Apr. 2021, doi: 10.1002/1873-3468.13995.
[3] H. Schägger and K. Pfeiffer, "Supercomplexes in the respiratory chains of yeast and mammalian mitochondria," *The EMBO Journal*, vol. 19, no. 8, pp. 1777–1783, Apr. 2000, doi: 10.1093/emboj/19.8.1777.

Preserving the Technological DNA of Electron Microscopy: The Vision of the Electron Microscopy Museum Nürnberg

Lukas E. Bochtler[1*], Katharina S. Bochtler[2]

[1]Electron Microscopy Museum Nürnberg (EMMN), Bucher Hauptstr. 47, 90427, Nürnberg, Germany
[2]Baylor College of Medicine, Neurological Research Institute, 1250 Moursund St., 77030, Houston, TX, USA

[*]info@em-museum.org

Electron microscopy has defined the modern era of structural and materials science, enabling discoveries ranging from viral ultrastructure to semiconductor nanofabrication. While instrumentation continues to advance rapidly, the systems that established the technical foundations of today's electron-optical platforms are increasingly being decommissioned. As laboratories modernize, critical developmental stages risk disappearing from the scientific record.

The Electron Microscopy Museum Nürnberg (EMMN) was founded to preserve and document the technological evolution of electron microscopy within its industrial and scientific context. Operating as a volunteer-driven initiative with a temporary exhibition space accessible by appointment, the museum maintains historically significant instruments in working condition wherever possible. In doing so, it preserves not only physical artifacts but also the operational principles underlying early electron-optical design.

The collection comprises landmark systems from major manufacturers including Siemens, Zeiss, Hitachi, and Philips. Among them is an early Zeiss EM8 platform, widely recognized as the first electron microscope incorporating a stigmator for the correction of lens astigmatism, marking a decisive advance in image quality and electron-optical control. Further milestones include the first Zeiss EM 912 omega-filtered TEM, representing a critical step in analytical transmission electron microscopy, and one of the oldest operational Hitachi TEM systems still functioning in Europe. An early Philips EM420 FEG, among the first field emission TEM systems, documents the transition toward high-brightness electron sources that define modern high-resolution microscopy. A Zeiss SESAM system developed in cooperation with the University of Tübingen and the Max Planck Institute for Solid State Research extends this continuum, linking foundational electron-optical design to contemporary aberration-corrected instrumentation.

Beyond preservation, the EMMN serves as a platform for dialogue between academia and industry, fostering continuity in technological innovation and offering an educational interface for students and early-career scientists. The long-term vision includes establishing a permanent exhibition and research-oriented documentation hub dedicated to the engineering and societal impact of the field. This initiative would integrate restoration, archival documentation, structured educational programs, and industry-supported exhibits within a coherent institutional framework.

As instrumentation cycles shorten and technological knowledge becomes increasingly digitized, maintaining access to the conceptual and material origins of the discipline constitutes both a scientific and cultural responsibility. The EMMN invites collaboration with academic institutions, industrial partners, and professional societies to ensure that foundational developments remain accessible, contextualized, and visible to future generations of microscopists, engineers, and instrument developers.

REMADE@ARI: A HUB FOR MATERIALS RESEARCH

Marta Lipińska-Chwałek[1,2*], Rafal. E. Dunin-Borkowski[1,2]

[1] Forschungszentrum Jülich GmbH, Ernst Ruska-Centre for Microscopy and Spectroscopy with Electrons, 52428 Jülich, Germany
[2] on behalf of the ReMade@ARI project team

[*]er-c@fz-juelich.de

As a result of the progressive depletion of natural resources, together with increasing waste, a cooperation aimed at shifting the global economy towards a circular economy is urgently needed. This change requires substantial research on materials that have high recycling potential, while exhibiting competitive functionalities.
To address this challenge, the most significant European analytical research infrastructures have joined forces in the ReMade@ARI Horizon Europe project, which provides a support hub for materials research while facilitating a step change to a circular economy.

ReMade@ARI offers comprehensive analytical services for research that focuses on the development of new materials for the circular economy [1]. The project offers coordinated access to over 50 research infrastructures across Europe, including electron microscopy facilities, synchrotrons, free electron lasers, neutron sources, high magnetic field laboratories, and ion or positron beam facilities (Fig.1). Senior scientists, facility experts and young researchers contribute scientific knowledge and extensive support to provide user services [2]. Particular attention is given to the implementation of comprehensive support mechanisms for researchers and developers from industry [3].

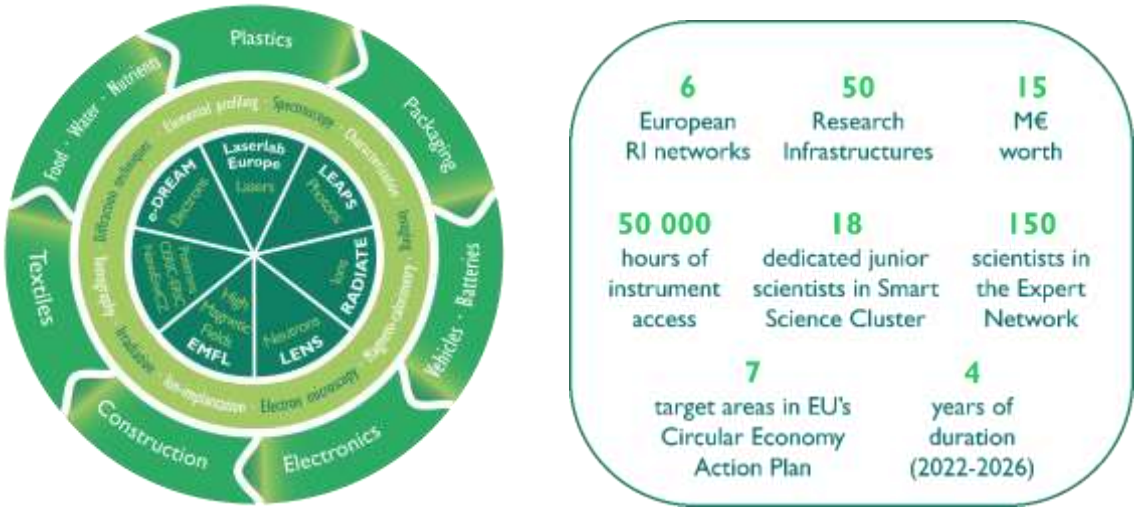

Fig. 1: Networks, topics, and techniques involved, together with the most important figures of the ReMade@ARI Horizon Europe project [4].

References:
[1] info@remade-project.eu (for general information)
[2] sciencesupport@remade-project.eu (for scientific support)
[3] industry@remade-project.eu (for industrial support)
[4] remade-project.eu

RIANA: RESEARCH INFRASTRUCTURE ACCESS IN NANOSCIENCE & NANOTECHNOLOGY

Marta Lipińska-Chwałek[1,2*], Rafal. E. Dunin-Borkowski[1,2]

[1] Forschungszentrum Jülich GmbH, Ernst Ruska-Centre for Microscopy and Spectroscopy with Electrons, 52428 Jülich, Germany
[2] on behalf of the RIANA project team

[*]er-c@fz-juelich.de

Research in the fields of nanoscience and nanotechnology is vital for a global sustainability. As the advancement in nanoscience and nanotechnology cannot be achieved without using research infrastructures (RI), the EU-funded RIANA project joined 7 European networks of top-level RIs providing access to the most advanced techniques relevant for nanofabrication, processing/synthesis, characterization and analytic as well as simulation capacity [1].
Highly customized and efficient access to 69 infrastructures, spread across 22 European countries (Fig.1), is coordinated via a single-entry point and enabled through comprehensive scientific and innovation service by senior scientists, facility experts and highly trained junior scientists. This core of RIANA is aligned to attract experienced and new users from academia or industry and will be prioritized for researchers with the brightest ideas and approach to make best use of the RI for nanoscience and nanotechnology in view of sustainability [2].
The excellence of user projects will be upheld by an independent review panel applying sharp evaluation criteria, in particular:

- scientific excellence,
- potential to technology readiness level increase
- level of cross-disciplinarity
- impact on safety for environment
- impact on nanoscience or nanotechnology.

RIANA will accept user proposals based on a “continuous call” that will be launched soon.

Networks:

LEAPS: synchrotron- and free-electron-laser based photon sources
Laserlab: laser sources
e-DREAM: electron microscopy
RADIATE: ion sources
LENS: neutron sources
EuroNanoLab: clean rooms
EUSMI: soft matter research infrastructures, NMR and high-power computing

Fig. 1: The RIANA consortium encompasses 7 networks (LEAPS, Laserlab, e-DREAM, RADIATE, LENS, EuroNanoLab and EUSMI) offering access to 69 infrastructures, spread across 22 European countries [1].

References:
[1] RIANA proposal - grant agreement No. 101130652
[2] RIANA-project.eu

Funded by the European Union